RSC Advances

This article can be cited before page numbers have been issued, to do this please use: F. Borges, E. Uriarte, L. Santana, A. Fonseca, M. J. Matos, J. Reis, M. Gutiérrez and Y. Duarte, *RSC Adv.*, 2016, DOI: 10.1039/C6RA05262B.

ROYAL SOCIETY OF CHEMISTRY

www.rsc.org/advances

View Article Online
DOI: 10.1039/C6RA05262B

RSC Advances

COMMUNICATION

Exploring coumarin potentialities: development of new enzymatic inhibitors based on the 6-methyl-3-carboxamidocoumarin scaffold

Received 00th January 20xx,
Accepted 00th January 20xx

DOI: 10.1039/x0xx00000x

www.rsc.org/

A. Fonseca[a,b], M. J. Matos[a], J. Reis[a], Y. Duarte[c], M. Gutiérrez[c], L. Santana[b], E. Uriarte[b] and F. Borges*[a]

Novel 6-methyl-3-carboxamidocoumarins (compounds 4-15) were synthesized by an effective three step synthetic strategy and screened towards MAO, AChE and BuChE enzymes. In general, the compounds act as selective MAO-B inhibitors. Compound 11 is highlighted as a potent (IC_{50} *h*MAO-B = 4.66 nM), reversible and non-competitive MAO-B inhibitor.

The increase in average life expectancy in developed countries has led to a rise of diagnosed cases of neurodegenerative diseases (ND's), namely Parkinson's (PD) and Alzheimer's (AD) diseases,[1,2] and dementia. Currently none of these illnesses have an effective treatment to modify or stop their progress. The drugs currently available are only useful for delay the progress of the diseases by controlling their symptoms.[2,3] Monoamine oxidases (MAOs) are enzymes present in the outer mitochondrial membrane, which have two isoforms named as MAO-A and MAO-B that catalyze the oxidation of biogenic amines.[4] Neurotransmitters, such as adrenaline, noradrenaline, dopamine, serotonin and β-phenylethylamine, are the main MAO substrates. Under normal conditions noradrenaline and serotonin are substrates of MAO-A while dopamine, a neurotransmitter present in low concentrations in the PD patients brain, has a greater affinity for MAO-B.[5] Activity of MAO-B is also linked to the production of reactive oxygen species (ROS) that cause oxidative stress and neuronal damage. Expression levels of MAO-B in neuronal tissue augment 4-fold with aging, resulting in an increased of dopamine metabolism and therefore, higher production of hydrogen peroxide (H_2O_2).[6] Thus, MAO-B inhibitors play an important role not only in dopamine metabolism but also in the reduction of brain oxidative damage. The involvement of MAO-B in AD is supported by the fact that neurons are extremely sensitive to oxidative stress as a consequence of: (a) their low content in endogenous antioxidants, such as glutathione, (b) the high proportion of an easily oxidized membrane covered by polyunsaturated fatty acids (c) the great oxygen brain consumption and also (d) a high content in iron.[7–9] In addition, concerning AD, MAO-B activity and the coproduction of H_2O_2 and other type of ROS are also increased, leading to an amplification of the neuron oxidative stress damage process. The current therapy for PD is only palliative and is focused in curtailing the motor symptoms by restoring the dopamine levels, namely by the administration of L-dopa, a dopamine precursor, alongside with other drug co-adjuvants, such as dopamine agonists, catechol-o-methyltransferase (COMT) and MAO-B inhibitors, such as selegiline. For AD, the therapy is only focused on the administration of acetylcholinesterase (AChE) inhibitors that target the cholinergic system, considering that the disease is characterized by a cholinergic neuronal loss, and consequently acetylcholine (ACh) depletion.[10] In brain synapses, ACh is hydrolyzed by AChE into choline and acetate.[11] At present butyrylcholinesterase (BuChE) was also proposed as a druggable target and as a result both enzymes represent putative therapeutic targets for improving the cholinergic deficit responsible for the decline in cognitive, behavioral and global functioning characteristic of AD.[12,13] Like in PD, none of the current drugs in therapy are able to modify disease progression, a condition that is well thought-out to be a driving force behind the ongoing research related to the discovery of new and potent inhibitors based on different types of scaffolds.[14]

Coumarins are heterocycles widely found in plants and other natural products that have synthetic accessibility and display remarkable biological properties, such as anticancer, antiviral, anti- inflammatory, antimicrobial and antioxidant agents.[15–29] Previous studies have shown that coumarin is a noteworthy scaffold for the discovery and development of new potent and selective MAO-B and AChE inhibitors.[25]

[a] CIQUP/Departamento de Química e Bioquímica, Faculdade de Ciências, Universidade do Porto, 4169-007, Porto, Portugal
[b] Departamento de Química Orgánica, Faculdade de Farmacia, Universidade de Santiago de Compostela, 15782, Santiago de Compostela, España
[c] Laboratorio de Síntesis Orgánica, Instituto de Química de Recursos Naturales Universidad de Talca, Casilla 747, 3460000, Talca, Chile.

View Article Online
DOI: 10.1039/C6RA05262B

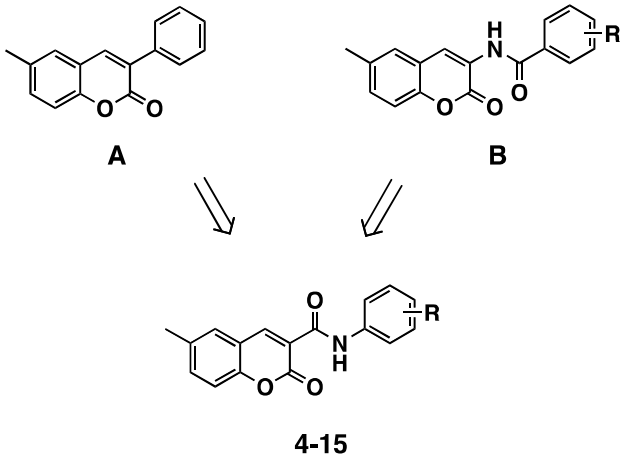

Figure 1 - Rational design followed in the present study to obtain the 3-substituted coumarins **4**-**15**.

Coumarins previously developed by our group (Figure **1**, structure A) have shown to display a remarkable potency and selectivity towards MAO-B activity. Till now our best-in-class coumarin IMAO-B was 3-(3-bromophenyl)-6-methylcoumarin (IC_{50} *h*MAO-B = 134 pM).[30] The data attained so far stimulate the progress of the project and in accordance a lead-optimization process was implemented in which the effect of a linker, located between the coumarin core and the exocyclic aromatic ring, in IMAO activity was studied. In addition, and taking advantage of the expenditure of the project it was also decided to move on from one-target to a dual-target drug design approach. So, other targets of interest in neurodegenerative diseases, like AChE, have been involved. The first studies were focused on the role of carbonylamine type linker (Figure 1, structure B). From the study, potent and selective IMAO-B were attained which were also able to inhibit AChE in the range from 12 µM to 69 µM.[29] The best dual candidate of the series was 3-(4'-chlorobenzamide)coumarin (IC_{50} *h*MAO-B = 1.95 µM and IC_{50} AChE = 18.71 µM). The best IMAO-B of the series was 3-(4'-methylbenzamide)-6-methylcoumarin (IC_{50} *h*MAO-B = 170 nM), which did not have relevant AChE inhibitory activity.

So, additional studies focused in the effect of a carboxamide linker, located between coumarin and the exocyclic aromatic substituent, were accomplished. Within this framework new 6-methyl-3-carboxamidocoumarins (compounds **4**-**15,** Figure 1) were designed, synthesized and studied as MAO enzymatic inhibitors.

Coumarin derivatives (**4**-**15**) have been obtained efficiently by a three step synthetic strategy described in Scheme **1** and explained in detail in supplementary material. Briefly, in the first step the coumarin used as starting material (compound **2**) was synthesized by a Knoevenagel condensation, in which 5-methylsalicylaldehyde (**1**) was refluxed with diethyl malonate in ethanol, in presence of catalytic amounts of piperidine. After subsequent hydrolysis, compound **3** was obtained with an overall yield of 89%.[31] Then, compounds **4**-**15** were synthesized by an amidation reaction in which the carboxylic acid **3** was activated with a coupling agent 1-ethyl-3-(3-dimethylaminopropyl)carbodiimide (EDC) in the presence of a nucleophilic catalyst 4-dimethylaminopyridine (DMAP).[32] After adding the primary aromatic amine with the desired substitution pattern, 6-methyl-3-carboxamidocoumarin derivatives (**4**-**15**) have been obtained with yields ranging from 56% to 83%. Structural characterization of the compounds was performed by ^{1}H and ^{13}C NMR spectroscopy, mass spectrometry (EI-MS) and elemental analysis and is included in supplementary material. The biological evaluation of the compounds **4**-**15** towards *h*MAO-A and *h*MAO-B was investigated by measuring their effects on the production of H_2O_2 from *p*-tyramine (a MAO substrate), using the Amplex Red MAO assay kit and recombinant *h*MAO with selegiline as reference compound.[33] In addition, the inhibitory activities of the compounds **4**-**15** were evaluated towards *Electrophorus electricus* AChE and bovine serum BuChE using Ellman spectrophotometric method and galantamine as reference compound.[34] The biological activity results expressed as IC_{50} values are listed in Table **1**.

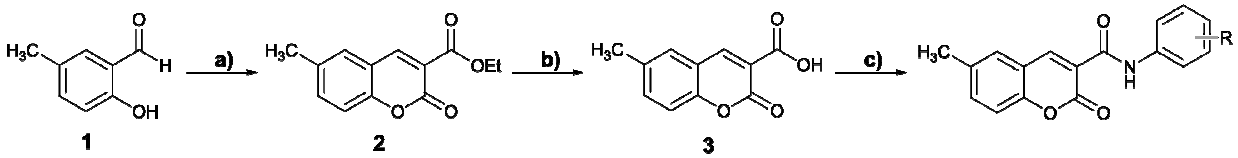

4 R= 2'-CH_3 **10** R= 2'-Br
5 R= 3'-CH_3 **11** R= 3'-Br
6 R= 4'-CH_3 **12** R= 4'-Br
7 R= 2'-OCH_3 **13** R= 2'-OH
8 R= 3'-OCH_3 **14** R= 3'-OH
9 R= 4'-OCH_3 **15** R= 4'-OH

Scheme 1 - Synthesis of coumarins **4**-**15**.Reagents and conditions: a) diethyl malonate, EtOH, piperidine, reflux, overnight. b) NaOH (0.5% aq./EtOH), reflux, 4h. c) EDC, DMAP, DCM, corresponding amine, 0 ºC to r.t., 4h.

View Article Online
DOI: 10.1039/C6RA05262B

Table 1. In vitro *h*MAO-A, *h*MAO-B and AChE inhibitory activities of 6-methyl-3-carboxamidocoumarin derivatives (**4-15**) and reference compounds.

Compound	IC_{50} (nM) *h*MAO-A	IC_{50} (nM) *h*MAO-B	SI	IC_{50} (μM) AChE
4	[a]	11.80 ± 1.10	>847.4 [b]	[c]
5	[a]	7.52 ± 1.05	>1329.8 [b]	535.24 ± 0.01
6	[a]	13.90 ± 1.30	>719.4 [b]	657.22 ± 0.01
7	[a]	160.60 ± 1.10	>62.3 [b]	494.45 ± 0.03
8	[a]	10.10 ± 1.20	>990.0 [b]	470.52 ± 0.18
9	[a]	296.90 ± 5.90	>33.7 [b]	[c]
10	[a]	13.50 ± 1.10	>740.7 [b]	621.23 ± 0.07
11	[a]	4.66 ± 1.13	>2145.9 [b]	591.44 ± 0.02
12	[a]	11.40 ± 1.20	>877.2 [b]	358.88 ± 0.05
13	[a]	18.30 ± 1.60	>546.4 [b]	666.37 ± 0.11
14	[a]	45.40 ± 1.30	>220.3 [b]	[c]
15	[a]	621.70 ± 1.80	>16.1 [b]	[c]
Selegiline	68730 ± 420	17.00 ± 1.90 [3]	4042.9	[d]
Galantamine	[d]	[d]	[d]	0.54 ± 0.50

[a] Inactive at 10 μM (highest concentration tested) [b] Values obtained under the assumption that the corresponding IC_{50} against MAO-A is the highest concentration tested (10 μM) [c] Inactive at 1000 μM (highest concentration tested) [d] Not determined

In general, compounds **4**-**15** display a remarkable selectivity towards *h*MAO-B, as they were inactive against *h*MAO-A at the highest concentration tested, and an interesting structure-dependent inhibitory potency. The methyl (**4**-**6**) and bromine (**10**-**12**) derivatives, bearing substituents located at *ortho*, *meta* and *para* positions of the exocyclic aromatic ring, exhibit MAO-B activity in the low nanomolar range. In the case of the methoxy substituted coumarins (compounds **7**-**9**), only the *meta*-substituted derivative display potency in the same range. For the hydroxy coumarin derivatives (compounds **13**-**15**), it can be concluded that the MAO-B inhibitory activity is strongly dependent on the substituent location, being enhanced when they are located at *ortho* and *meta* positions. In summary, it was observed that the presence of electron donor substituents in the *para* position of the aryl ring attached to the amide group lead to a potency decrease, whereas derivatives bearing weak electron donors or acceptors do not change IMAO-B potency independently of their position. The 6-methyl-3-carboxamidocoumarins substituted in the *meta* position (compounds **5**, **8** and **11**) have a superior activity towards MAO-B than their *ortho* (compounds **4**, **7** and **10**) and *para* (compounds **6**, **9** and **12**) counterparts. In particular, compounds **5** (IC_{50} *h*MAO-B = 7.52 nM) and **11** (IC_{50} *h*MAO-B = 4.66 nM) showed *h*MAO-B inhibition at a low nanomolar range, slightly better than selegiline, and also benefiting from an excellent selective profile.

To examine the type of inhibition mechanism of the most promising *h*MAO-B inhibitor (compound **11**) kinetic experiments were performed. For this purpose, the initial rates of the MAO-B-catalyzed oxidation of *p*-tyramine at five different substrate concentrations, in the absence or presence of the selected coumarin inhibitor, at different concentrations, were measured. The results are depicted in Figure **2**.

Graphical analyses of the reciprocal Lineweaver−Burk plots allow the determination of Michaelis−Menten reaction kinetic parameters (Michaelis constant, K_m and maximum velocity, V_{max}). Concerning compound **11**, it was found that the K_m remained almost constant at different concentrations of the inhibitor whereas V_{max} decreased. The Lineweaver-Burk plots obtained for different concentrations of compound **11** (Figure **2**) displayed a series of converging lines on the same point of the x-axis (1/[S]) profiling a non-competitive inhibition mechanism. From the Dixon plots, obtained from the replots of the slopes of the Lineweaver–Burk plots *vs* inhibitor concentrations (upper right corner), the *h*MAO-B inhibition binding affinities, determined as inhibition constants (*Ki*), were calculated. As a result, compound **11** (Figure 2) displayed a *Ki* value of 2.70 nM. The estimated *Ki* value correlated well with the inhibition mechanism suggested by the kinetic experiments, with the compound displaying IC_{50} and *Ki* values slightly different but within the low nanomolar range.

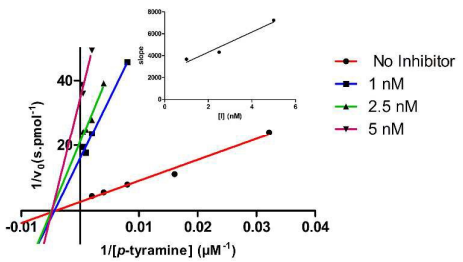

Figure 2 - Kinetic study on the mechanism of *h*MAO-B inhibition by compound **11**. The effect of the inhibitors on the enzyme was determined from the double reciprocal plot of 1/rate (1/V) versus 1/substrate concentration in presence of varying concentrations of the inhibitors. The *Ki* value was calculated by the intersection of the curves obtained by plotting 1/V versus the inhibitor concentration for each substrate concentration (Dixon plots insets on the top right).

View Article Online
DOI: 10.1039/C6RA05262B

The reversibility of MAO-B inhibition by the test compound **11** was then assessed by time-dependent inhibition studies. The behavior of standard irreversible (R-(-)-deprenyl) and reversible (safinamide) inhibitors was also evaluated under the same experimental conditions. MAO-B activity (% of control) was measured along 60 minutes incubation with the enzyme inhibitors (Figure **3**). The analysis of time-dependent enzyme inhibition studies performed with the irreversible inhibitor (R-(-)-deprenyl, Figure **3**) showed that the enzyme residual activity decayed continuously after the first 15 minutes of incubation, which is consistent with irreversible enzymatic inhibition. In case of the reversible inhibitor safinamide (Figure **3**), an enhancement on enzymatic activity was observed along the analysis time. A similar behavior was observed for compound **11**, which shows the gradual link to the allosteric binding site (non-competitive inhibitor) in the first 15 minutes, proceeded by the enhancement of enzymatic activity along the last 60 minutes, as its expectable of a MAO-B reversible inhibition profile.

penetration was also calculated. The data are presented in Table **2**. Complete procedures of *in vitro* biological studies, statistical analysis and drug-like properties calculations are listed in the supplementary material.

Analyzing the results for the inhibitory activity towards human AChE depicted in Table 1, one can conclude that all compounds presented a moderate inhibitory activity (micromolar range) towards the enzyme. None of the tested compounds displayed a noticeable activity towards BuChE at the highest concentration tested (10 mM) (data not shown). Compound **12**, the *para*-bromine coumarin derivative, was found to be the most active compound towards AChE (IC_{50} = 358.88 µM). Analysing the overall data, one can conclude that the 6-methyl-3-carboxamidocoumarins substituted with a hydroxyl substituent (compounds **13**-**15**) are the less potent compounds of the series. However, when a methyl or methoxy substituent (compounds **5** and **8**) is located at *meta* position of the aromatic exocyclic ring a slight increment of inhibitory activity is observed, when compared with their *ortho* (compounds **4** and) and *para* (compounds **6** and **9**) counterparts.

Table 2. Drug-like properties of 6-methyl-3-carboxamidocoumarin derivatives (**4-15**) and reference compounds.

Compound	Molecular weight	cLogP	TPSA (Å^2)	H-bond donor	H-bond acceptor	Volume (Å^3)
4 / 5 / 6	293.3	3.66/ 3.68 / 3.71	59.31	4	1	264.5
7/ 8 / 9	309.3	3.27/ 3.29 / 3.31	68.54	5	1	273.5
10/ 11 / 12	358.2	4.02/ 4.04 / 4.07	59.31	4	1	265.8
13/ 14/ 15	295.3	2.99/ 2.75 / 2.78	79.54	5	2	256.0
Selegiline	187.3	2.64	3.24	1	0	202.6
Galantamine	287.4	1.54	41.93	4	1	268.2

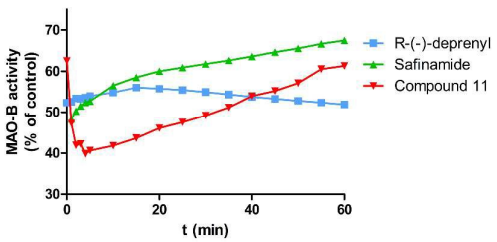

Figure 3 - Time-dependent inhibition of recombinant human MAO-B by standard compounds (R)-(−)-Deprenyl (50 nM), safinamide (40 nM) and test compound **11** (15 nM), The remaining activity was expressed as % of activity. Data are the mean ± S.D. of three different experiments.

Finally, the drug-like properties of the compounds **4–15**, namely the lipophilicity (expressed as the octanol/water partition coefficient, and herein called clogP) and other properties (molecular weight, number of hydrogen acceptors and donors and volume) were calculated using the Molinspiration calculation software. Topological polar surface area (TPSA) that has been shown to be a very good descriptor of drug absorption, including intestinal absorption, bioavailability, Caco-2 permeability and blood–brain barrier

In our previous study, compound **6** analogue (compound **4** in ref.29), which also have a methyl substituent, in *para* position, had displayed a IC_{50} *h*MAO-B = 170 nM, which is ten times lower. Nevertheless, it showed a superior affinity to AChE than the compounds presented here.[29] Thus, it can be concluded that the carboxamide spacer, and specially the location of the carbonyl group, is a key feature for MAO-B and AChE inhibitory activities.

Additionally, from the prediction drug-like properties of compounds **4-15** (Table **2**) it can be observed that no violations of Lipinski's rule (molecular weight, logP, number of hydrogen donors and acceptors) were found and that the TPSA, described as a predictive indicator of the drug capacity of membrane penetration, is favorable. Therefore, the data provided a preliminary indication that this type of compounds can cross membranes and act in the central nervous system.

The remarkable results found for compounds **5** and **11** (*h*MAO-B IC_{50} of 7.52 and 4.66 nM respectively) encourage us to continue our research based on the coumarin scaffold. Compound **11** acts as a potent, selective, reversible and non-competitive MAO-B inhibitor. In addition, compound **12** (*h*MAO-B IC_{50} of 11.40 nM and AChE IC_{50} of 358.88 µM) can be looked as a stimulating framework to develop dual target MAO-B/AChE inhibitors. Further examination of the cytotoxic

View Article Online
DOI: 10.1039/C6RA05262B

and pharmacokinetic properties of compounds **11** and **12** is important to define if which of them will be a candidate for in vivo studies. In summary, the data attained so far is a noteworthy contribution for the development of new drug candidates for PD and AD based on 6-methylcoumarin scaffold.

Notes and references

1 R. J. Castellani, R. K. Rolston and M. a. Smith, *Disease-a-Month*, 2010, **56**, 484–546.

2 L. M. L. de Lau and M. M. B. Breteler, *Lancet. Neurol.*, 2006, **5**, 525–535.

3 M. R. Farlow and J. L. Cummings, *Am. J. Med.*, 2007, **120**, 388–397.

4 J. P. Johnson, *Biochem. Pharmacol.*, 1968, **17**, 1285–1297.

5 M. B. Youdim, D. Edmondson and K. F. Tipton, *Nat Rev Neurosci.*, 2006, **7**, 295–309.

6 A. Gaspar, N. Milhazes, L. Santana, E. Uriarte, F. Borges and M. J. Matos, *Curr. Top. Med. Chem.*, 2015, **15**, 432–445.

7 P. Riederer, *Neurotoxicology*, 2004, **25**, 271–277.

8 V. Jain, M. C. Langham and F. W. Wehrli, *J. Cereb. Blood Flow Metab.*, 2010, **30**, 1598–1607.

9 T. A. Rouault, *Nat Rev Neurosci.*, 2013, **14**, 551–564.

10 M. Itakura, H. Nakajima, T. Kubo, Y. Semi, S. Kume, S. Higashida, A. Kaneshige, M. Kuwamura, N. Harada, A. Kita, Y.-T. Azuma, R. Yamaji, T. Inui and T. Takeuchi, *J. Biol. Chem.*, 2015, jbc.M115.669291.

11 V. N. Talesa, *Mech. Ageing Dev.*, 2001, **122**, 1961–1969.

12 M. Khoobi, M. Alipour, A. Moradi, A. Sakhteman, H. Nadri, S. F. Razavi, M. Ghandi, A. Foroumadi and A. Shafiee, *Eur. J. Med. Chem.*, 2013, **68**, 291–300.

13 R. M. Lane, S. G. Potkin and A. Enz, *Int. J. Neuropsychopharmacol.*, 2006, **9**, 101–124.

14 M. Singh, M. Kaur, H. Kukreja, R. Chugh, O. Silakari and D. Singh, *Eur. J. Med. Chem.*, 2013, **70**, 165–188.

15 F. Borges, F. Roleira, N. Milhazes, L. Santana and E. Uriarte, *Curr. Med. Chem.*, 2005, **12**, 887–916.

16 F. Borges, F. M. F. Roleira, N. Milhazes, E. Uriarte and L. Santana, *Front. Med. Chem.*, 2009, **4**, 23–85.

17 M. Riveiro, N. De Kimpe, A. Moglioni, R. Vazquez, F. Monczor, C. Shayo and C. Davio, *Curr. Med. Chem.*, 2010, **17**, 1325–1338.

18 M. J. Matos, S. Vazquez-Rodriguez, L. Santana, E. Uriarte, C. Fuentes-Edfuf, Y. Santos and A. Munoz-Crego, *Med. Chem. (Los. Angeles).*, 2012, **8**, 1140–1145.

19 D. Viña, M. J. Matos, G. Ferino, E. Cadoni, R. Laguna, F. Borges, E. Uriarte and L. Santana, *ChemMedChem*, 2012, **7**, 464–470.

20 M. J. Matos, S. Vazquez-Rodriguez, E. Uriarte, L. Santana and D. Viña, *Bioorg. Med. Chem. Lett.*, 2011, **21**, 4224–4227.

21 D. Secci, S. Carradori, A. Bolasco, P. Chimenti, M. Yáñez, F. Ortuso and S. Alcaro, *Eur. J. Med. Chem.*, 2011, **46**, 4846–4852.

22 S. Vazquez-Rodriguez, M. J. Matos, L. Santana, E. Uriarte, F. Borges, S. Kachler and K. N. Klotz, *J. Pharm. Pharmacol*, 2013, **65**, 697-703.

23 I. Kostova, S. Bhatia, P. Grigorov, S. Balkansky, V. S. Parmar, A. K. Prasad and L. Saso, *Curr. Med. Chem.*, 2011, 18, 3929–3951.

24 M. J. Matos, P. Janeiro, R. M. González Franco, S. Vilar, N. P. Tatonetti, L. Santana, E. Uriarte, F. Borges, J. A. Fontenla and D. Viña, *Future Med. Chem.*, 2014, **6**, 371–383.

25 M. J. Matos, D. Viña, E. Quezada, C. Picciau, G. Delogu, F. Orallo, L. Santana and E. Uriarte, *Bioorg. Med. Chem. Lett.*, 2009, **19**, 3268–3270.

26 M. J. Matos, D. Viña, C. Picciau, F. Orallo, L. Santana and E. Uriarte, *Bioorg. Med. Chem. Lett.*, 2009, **19**, 5053-5055.

27 M. J. Matos, S. Vazquez-Rodriguez, L. Santana, E. Uriarte, C. Fuentes-Edfuf, Y. Santos and A. Muñoz-Crego, *Molecules*, 2013, **18**, 1394–1404.

28 M. J. Matos, C. Terán, Y. Pérez-Castillo, E. Uriarte, L. Santana and D. Viña, *J. Med. Chem.*, 2011, **54**, 7127–7137.

29 D. Viña, M. J. Matos, M. Yáñez, L. Santana and E. Uriarte, *Med. Chem. Commun.*, 2012, **3**, 213–218.

30 M. J. Matos, S. Vilar, V. Garcia-Morales, N. P. Tatonetti, E. Uriarte, L. Santana and D. Viña, *ChemMedChem*, 2014, **9**, 1488–1500.

31 F. Chimenti, B. Bizzarri, A. Bolasco, D. Secci, P. Chimenti, A. Granese, S. Carradori, D. Rivanera, A. Zicari, M. Scaltrito, and F. Sisto, *Bioorg. Med. Chem. Lett.* 2010, **20**, 4922–4926.

32 C. Murata, T. Masuda, Y. Kamochi, K. Todoroki, H. Yoshida, H. Nohta, M. Yamaguchi and A. Takadate, *Chem. Pharm. Bull. (Tokyo).* 2005, **53**, 750–758.

33 M. Yáñez, N. Fraiz, E. Cano and F. Orallo, *Biochem. Biophys. Res. Commun.* 2006, **344**, 688–695.

34 P. Torre, L. Saavedra, J. Caballero, J. Quiroga, J. Alzate-Morales, M. Cabrera and J. Trilleras, *Molecules* 2012, **17**, 12072–12085